
Two-band quantum models for semiconductors arising from the Bloch envelope theory

Giuseppe Ali¹, Giovanni Frosali², and Omar Morandi³

¹ Istituto per le Applicazioni del Calcolo “M. Picone”, CNR - Via P. Castellino 111, I-80131 Napoli, Italy, and INFN-Gruppo c. Cosenza g.ali@iac.cnr.it

² Dipartimento di Matematica Applicata “G.Sansone”, Università di Firenze - Via S.Marta 3, I-50139 Firenze, Italy giovanni.frosali@unifi.it

³ Dipartimento di Elettronica e Telecomunicazioni, Università di Firenze - Via S.Marta 3, I-50139 Firenze, Italy omar.morandi@unifi.it

1 Introduction

In the recent past, the interest in quantum hydrodynamic models for semiconductors has increased considerably. In fact, classical fluid dynamical models fail to be adequate for new generations of semiconductor devices, where quantum effects tend to become not negligible or even dominant (see [6] and the references therein). This paper is particularly devoted to multi-band quantum models, introduced to describe the Resonant Interband Tunneling Diode (RITD) [5, 11]. In section 2 we review briefly two-band quantum models for semiconductors arising from the Bloch envelope theory [7, 10]. In section 3 we present a new Madelung-like hydrodynamical formulation for the previous models, based on a suitable definition of osmotic and current velocities. This method has been applied in [1] to the Kane model. We conclude this paper with a thorough physical discussion of the models, with some numerical experiments showing the different description of the interband resonant tunneling of the previous models.

2 The envelope function models

In quantum mechanics the motion of an electron is described by a quantum Hamiltonian operator, which governs the evolution of a wave function Ψ , whose modulus $n(x, t) := |\Psi(x, t)|^2$ represents the probability density of finding the electron at the position x and time t . Since we are interested in modeling multi-band quantum effects, it is necessary to introduce quantum densities for each band, with a possibly clear physical meaning. Then, the tunneling process will be described by an operator which is non-diagonal with respect to the band index. In view of this, the effective mass formalism,

and in particular the $\mathbf{k}\cdot\mathbf{p}$ envelope function method, seems to be the natural framework for multi-band analysis [12].

The basic idea behind $\mathbf{k}\cdot\mathbf{p}$ theory is that we do not need to calculate the evolution of the full wave function to obtain the trajectory of an electron through the crystal but it is sufficient to calculate the evolution of the so-called envelope function, a smooth function which is obtained by replacing Ψ by its average in each primitive cell. So, the microscopic structure of the full wave function is not relevant.

The application of the $\mathbf{k}\cdot\mathbf{p}$ theory gives rise to models which differ both by the choice of the set of basis functions, and by the approximation procedure. Generally speaking, $\mathbf{k}\cdot\mathbf{p}$ models arise from perturbative methods where the crystal momentum \mathbf{k} is considered a “small” quantity. Typically, this analysis applies when $k = 0$ is a stationary point (the Γ point) for the dispersion relation of the band, since the momentum of the electron is localized around this point. Different sets of basis functions are generated by using suitable projection operators on the Bloch basis in such a way that the new basis elements “approach” the original Bloch waves as $|k|$ tends to zero. The most common choice of $\mathbf{k}\cdot\mathbf{p}$ basis was proposed by Kane (in its pioneering paper of 1956 [7]) with the aim of approximating the periodic part of each Bloch function by its value at the Γ point. In spite of its simplicity, this choice fails to give an adequate physical interpretation of tunneling phenomena. To overcome this difficulty, other choices have been proposed in literature [9]. In particular, in this paper, we refer to the Multi-band Envelope Function (MEF) model [10].

Since every $\mathbf{k}\cdot\mathbf{p}$ model involves a full coupling among all unperturbed bands, to retain only those terms which are well localized into the bands of interest, a cutoff is employed in the expansion of the solution Ψ . In semiconductor devices, the current is mainly generated by transport of electrons in conduction band and in light hole valence band, thus it is customary to approximate the wave function Ψ solely by its conduction and valence components, denoted here ψ_c and ψ_v , respectively.

Irrespectively of the choice of the basis, the conduction and valence components are determined by solving a Schrödinger-like equation of the form

$$i\hbar\frac{d}{dt}\begin{pmatrix} \psi_c \\ \psi_v \end{pmatrix} = H\begin{pmatrix} \psi_c \\ \psi_v \end{pmatrix}, \quad (1)$$

where H is an approximation of a full-band Hamiltonian. Its diagonal components correspond to uncoupled bands, and the off-diagonal terms account for interband effects. This type of approximation can be performed in different ways [4], and the method of approximating the Bloch basis affects the specific form of H deeply, not only from a formal point of view, but also from a physical one.

Using the classical Kane basis, Ψ can be approximated by

$$\Psi(x, t) \simeq \psi_c^K(x, t)u_c^K(x) + \psi_v^K(x, t)u_v^K(x). \quad (2)$$

Here, u_a^K is the periodic part of the Bloch function $b_a(k, x)$, $a = c, v$, evaluated at $k = 0$. Instead, the MEF model uses an expansion in the Wannier basis, approximating the conduction and valence components up to the first order in $|k|$ [10]. Then, Ψ can be approximated by

$$\Psi(x, t) \simeq \psi_c^M(x, t)u_c^M(x) + \psi_v^M(x, t)u_v^M(x). \quad (3)$$

It is well known that each Wannier basis element arises from applying the Fourier transform to the Bloch functions related to the same band index n . The envelope functions ψ_c^M and ψ_v^M are the projections of Ψ on the Wannier basis, and therefore the corresponding multi-band densities represent the (cell-averaged) probability amplitude of finding an electron on the conduction or valence bands, respectively.

This simple picture does not apply to the Kane model. In fact, in the Kane approach, the periodic part $u_n(k, x)$ of each element of the Bloch basis, $b_n(k, x) = e^{ikx}u_n(k, x)$, is projected on the same basis but calculated for $k = 0$. Thus, the generic element of the Kane basis, defined by $b_n^K(k, x) = e^{ikx}u_n^K(0, x)$, is no more linked to the Bloch basis by a diagonal transformation. This fact can be simply verified by introducing a unitary operator $\Theta_{n,n'}$ such that $u_n(k, x) = \sum_{n'} \Theta_{n,n'}(k)u_{n'}^k(0, x)$. Then, we have

$$b_n(k, x) = e^{ikx}u_n(k, x) = \sum_{n'} e^{ikx}\Theta_{n,n'}(k)u_{n'}^k(0, x) = \sum_{n'} \Theta_{n,n'}(k)b_{n'}^K(k, x).$$

$\Theta_{n,n'}$ written for two bands and approximated up to the first order in $|k|$ is

$$\Theta_{n,n'}(k) = \delta_{n,n'} + \frac{\hbar^2}{m_0} \sum_{n \neq n'} \frac{P_{n,n'}}{E_n - E_{n'}} k. \quad (4)$$

At the envelope function level, (4) implies that Kane envelope functions and MEF envelope functions are connected by the relation $\psi_a^K = \sum_b \Theta_{b,a}\psi_b^M$. Using transformation (4) at the first order in $|k|$, we can write explicitly [10]

$$\psi_a^K = \psi_a^M + i \frac{\hbar^2}{m_0} \sum_{b \neq a} \frac{P_{a,b}}{E_a - E_b} \nabla \psi_b^M. \quad (5)$$

Going back to (1), for the Kane model the Hamiltonian takes the form

$$H = H^K := \begin{pmatrix} -\frac{\hbar^2}{2m_0}\Delta + E_c + V & -\frac{\hbar^2}{m_0}P \cdot \nabla \\ \frac{\hbar^2}{m_0}P \cdot \nabla & -\frac{\hbar^2}{2m_0}\Delta + E_v + V \end{pmatrix}, \quad (6)$$

where E_c is the minimum of the conduction band energy, E_v is the maximum of the valence band energy, m_0 is the bare electron mass and $P := P_{c,v}$ is the

coupling coefficient between the two bands given by the matrix element of the gradient operator between u_c^K and u_v^K [7, 3].

For the MEF model in a semiconductor with isotropic effective mass tensor, the Hamiltonian is

$$H = H^M := \begin{pmatrix} -\frac{\hbar^2}{2m_c^*}\Delta + E_c + V & -\frac{\hbar^2 P \cdot \nabla V}{m_0 E_g} \\ -\frac{\hbar^2 P \cdot \nabla V}{m_0 E_g} & \frac{\hbar^2}{2m_v^*}\Delta + E_v + V \end{pmatrix}, \quad (7)$$

where $E_g = E_c - E_v$ and m_c^* , m_v^* are the effective masses for the conduction and valence bands, respectively. In the following we will assume $m_c^* = m_v^* = m^*$ and, for simplicity, we will focus on one-dimensional systems.

3 Hydrodynamic models

In this section, following the technical procedure proposed in [1], we compare the hydrodynamic formulations of the Kane and MEF models.

In general, we expect a straightforward extension of the hydrodynamical formalism for a single-band semiconductor to multi-band framework, provided that each component of the wave function behaves like the electron wave function in a single-band whenever no interband effects are present.

In this work we apply the WKB method, which is a standard way to write the Schrödinger equation in hydrodynamic form [6]. Extending this approach to two-band models, we look for solutions to the system (1), written with $H = H^A$, $A = K, M$ (see (6) and (7)), of the form

$$\psi_a^A(x, t) := \sqrt{n_a^A(x, t)} \exp\left(\frac{im^A}{\hbar} S_a^A(x, t)\right), \quad a = c, v, \quad (8)$$

with $m^K = m_0$, $m^M = m^*$. In the following, we will not specify the attributions of the indices a and A . The squared amplitude n_a^A can be immediately regarded as a probability density of the electron in the band a , and the gradient of the phase corresponds to the velocity of the electron in the same band. We remark that both $n_c^M + n_v^M = |\psi_c^M|^2 + |\psi_v^M|^2$ and $n_c^K + n_v^K = |\psi_c^K|^2 + |\psi_v^K|^2$ can be interpreted as approximations of the true total density number of electrons, which in principle are different, due to the different type of expansion used in the Kane and MEF approaches. Using (8), we can transform system (1), written with $H = H^A$, for the variables ψ_a^A , to a formally equivalent system for the variables n_a^A , S_a^A . To derive a hydrodynamical formulation of (1), we introduce the complex velocities $u_a^A := \frac{\hbar}{m^A} \nabla \log \psi_a^A$, and write

$$u_a^A = u_{\text{os},a}^A + iu_{\text{el},a}^A := \frac{\hbar}{m^A} \frac{\nabla \sqrt{n_a^A}}{\sqrt{n_a^A}} + i\nabla S_a^A. \quad (9)$$

The real and imaginary parts of u_a^A are named osmotic velocities and current velocities, respectively. Also, we introduce the electron current densities $J_a^A := \frac{\hbar}{m^A} \text{Im} (\psi_a^A \nabla \psi_a^A) = n_a^A u_{\text{el},a}^A$ and the interband particle densities $n_{cv}^A = \overline{n_{vc}^A} = \overline{\psi_c^A \psi_v^A} = \sqrt{n_c^A} \sqrt{n_v^A} e^{i\sigma^A}$, with $\sigma^A := \frac{m^A}{\hbar} (S_v^A - S_c^A)$.

Using the above definitions in (1), we can derive equations for the particle densities n_c^A , n_v^A , and the currents J_c^A , J_v^A ,

$$\frac{\partial n_c^A}{\partial t} + \nabla \cdot J_c^A = S_{cv}^A, \quad \frac{\partial n_v^A}{\partial t} + \alpha \nabla \cdot J_v^A = S_{vc}^A, \quad (10)$$

$$\frac{\partial J_c^A}{\partial t} + \text{div} \left(\frac{J_c^A \otimes J_c^A}{n_c^A} \right) + \frac{n_c^A}{m^A} \nabla (E_c + V + V_c^A + V_{cv}^A) = S_{cv}^A \frac{J_c^A}{n_c^A}, \quad (11)$$

$$\frac{\partial J_v^A}{\partial t} + \alpha \text{div} \left(\frac{J_v^A \otimes J_v^A}{n_v^A} \right) + \frac{n_v^A}{m^A} \nabla (E_v + V + \alpha V_v^A + V_{vc}^A) = S_{vc}^A \frac{J_v^A}{n_v^A}, \quad (12)$$

with $\alpha = 1$ for the Kane model and -1 for the MEF model. Here, $V_a^A = -\frac{\hbar^2 \Delta \sqrt{n_a^A}}{2m^A \sqrt{n_a^A}}$ are the Bohm potentials for each band, the interband potentials V_{ab}^A are given by

$$\begin{aligned} V_{cv}^K &= -\hbar \text{Re} \left(\frac{n_{cv}^K P \cdot u_v^K}{n_c^K} \right), & V_{vc}^K &= \hbar \text{Re} \left(\frac{n_{vc}^K P \cdot u_c^K}{n_v^K} \right), \\ V_{cv}^M &= V_{vc}^M = -\frac{\hbar^2 P \cdot \nabla V}{m_0 E_g n_c^M} \text{Re} n_{cv}^M, \end{aligned}$$

and we have introduced

$$\begin{aligned} S_{cv}^K &= -2 \text{Im} (n_{cv}^K P \cdot u_v^K), & S_{vc}^K &= 2 \text{Im} (n_{vc}^K P \cdot u_c^K), \\ S_{cv}^M &= -S_{vc}^M = -\frac{2\hbar P \cdot \nabla V}{m_0 E_g} \text{Im} n_{cv}^M. \end{aligned}$$

In order to close the system and obtain an extension of the classical Madelung fluid equations, we need to add an equation for σ^A ,

$$\frac{\hbar}{m^A} \nabla \sigma^A = \frac{J_v^A}{n_v^A} - \frac{J_c^A}{n_c^A}. \quad (13)$$

Summing the equations for the densities, we obtain the balance law for the total density (continuity equation). We see that for the MEF model, the total current is the sum of the currents for valence and conduction band. In the Kane model, the continuity equation reads

$$\frac{\partial}{\partial t} (n_c^K + n_v^K) + \nabla \cdot (J_c^K + J_v^K + 2 \frac{\hbar}{m_0} P \text{Im} n_{cv}^K) = 0.$$

The appearance of an additional interband term for the current is an indication of the inadequacy of the Kane-based hydrodynamical model. This topic will be discussed in details in the following section.

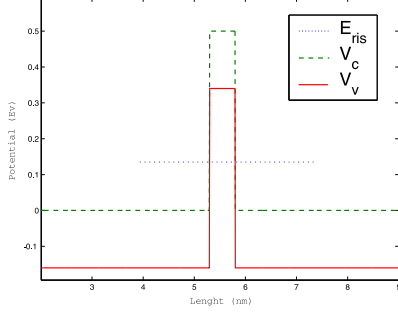


Fig. 1. Band diagram of the simulated heterostructure. The dotted line denotes the energy of the resonant state in the valence quantum well.

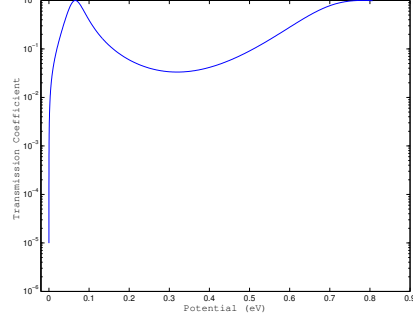


Fig. 2. Plot of the transmission coefficient of the heterostructure as a function of the E_{inc}

4 Numerical results

In this section we show some numerical results arising from the two proposed approaches. Our aim is to show that a more direct physical meaning can be ascribed to the hydrodynamical variables derived from the MEF approach.

We consider a heterostructure which consists of two homogeneous regions separated by a potential barrier and which realizes a single quantum well in valence band. In figure 1 we have marked the energy of resonant state $E_{ris} = 0.066 \text{ eV}$, which is given by the solution of an eigenvalue problem for the Hamiltonian operator. In our simulation, we have used the following parameters: $E_g = E_c - E_v = 0.16 \text{ eV}$, $m^* = 0.023 m_0$, $P = 5 \cdot 10^9 m^{-1}$.

A conduction electron beam (i.e. a plane wave envelope function with positive momentum k and energy $\hbar^2 k^2 / 2m^* + E_c$) is injected in the heterostructure from the left. Then, the analytical solution for eq. (1) in the regions $x < 0$ and $x > L$ is explicitly given by $\psi = e^{-iE_{inc}t/\hbar} \psi^A$ where

$$\psi^A = \begin{cases} \mathbf{e}_c^A \{ e^{ikx} + r_c e^{-ikx} \} + \mathbf{e}_v^A r_v e^{ik_{rv}x}, & x \in (-\infty, 0] \\ \mathbf{e}_c^A t_c e^{ikx} + \mathbf{e}_v^A t_v e^{-ik_{rv}x}, & x \in [L, \infty) \end{cases} \quad A = M, K$$

where $\psi^A = \begin{pmatrix} \psi_c^A \\ \psi_v^A \end{pmatrix}$, $k_{rv} = -\frac{i}{\hbar} \sqrt{2m^*(E_{inc} - E_v)}$, and \mathbf{e}_c^A , \mathbf{e}_v^A are unitary vectors defined as follows: $\mathbf{e}_c^M = \begin{pmatrix} 1 \\ 0 \end{pmatrix}$, $\mathbf{e}_v^M = \begin{pmatrix} 0 \\ 1 \end{pmatrix}$ for the MEF model, and

$$\mathbf{e}_c^K = \begin{pmatrix} \sqrt{\frac{\sqrt{\eta} + E_g}{2\sqrt{\eta}}} \\ i\sqrt{\frac{\sqrt{\eta} - E_g}{2\sqrt{\eta}}} \end{pmatrix}, \quad \mathbf{e}_v^K = \begin{pmatrix} \sqrt{\frac{\sqrt{\eta} - E_g}{2\sqrt{\eta}}} \\ -i\sqrt{\frac{\sqrt{\eta} + E_g}{2\sqrt{\eta}}} \end{pmatrix}, \quad \text{with } \eta = E_g^2 + 4\frac{\hbar^2 k^2 P^2}{m_0^2},$$

for the Kane model. Furthermore, $r_c(t_c)$ and $r_v(t_v)$ are the reflection (transmission) coefficients in the conduction and valence bands, respectively. They depend

on the detailed shape of the heterostructure, and are numerically evaluated by a Runge-Kutta scheme which solves directly the eigenvalue problem related to eq. (1), obtained, as usual, by formally replacing $i\hbar\frac{d}{dt}$ with E [8].

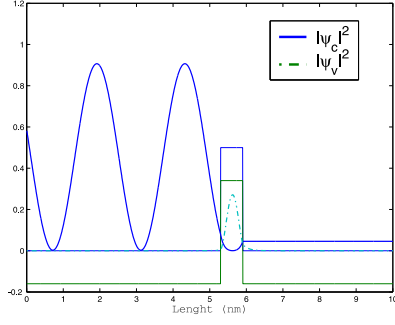


Fig. 3. MEF model: $E_{inc} = 0.028$ eV

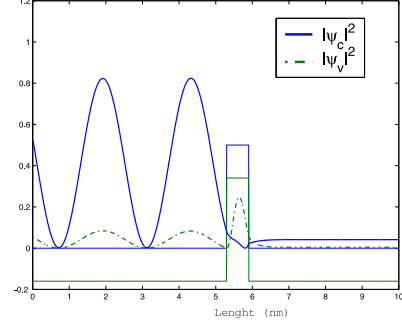


Fig. 4. Kane model: $E_{inc} = 0.028$ eV

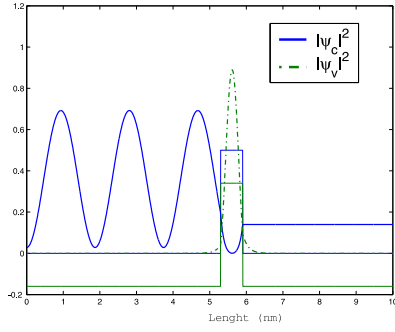


Fig. 5. MEF model: $E_{inc} = 0.046$ eV

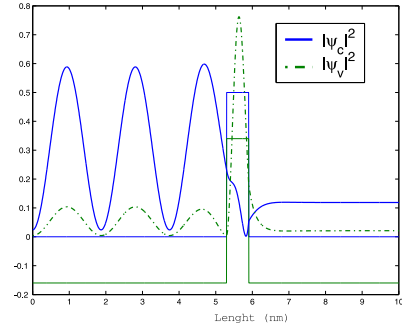


Fig. 6. Kane model: $E_{inc} = 0.046$ eV

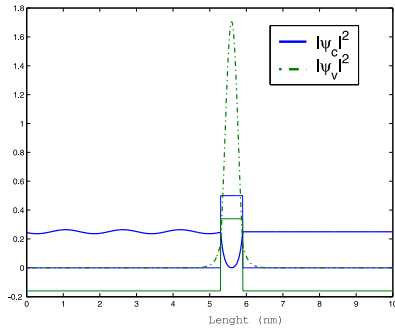


Fig. 7. MEF model: $E_{inc} = 0.066$ eV

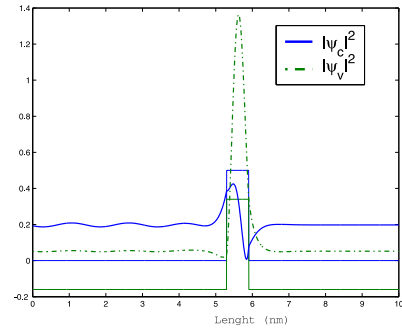


Fig. 8. Kane model: $E_{inc} = 0.066$ eV

We calculate the envelope function solution in the region $0 < x < L$ for incremental values of the electron beam energy. The results are plotted in figures 3-8 (left-hand side for the MEF model, and right-hand side for the Kane model).

When the electron energy is well below of the resonant energy E_{ris} (fig. 3-4) the incident conduction plane wave is reflected: r_c approaches 1 and, consequently, the transmission coefficient t_c tends to 0. In this case the valence states are almost unexcited and a small amount of charge cumulates in the valence quantum well. Instead, when the electron energy approaches the resonant level, the transmission coefficient enhances and the electron can travel from the left to the right of the heterostructure by using the bounded valence resonant state as a “bridge” state. Identifying ψ_c^M and ψ_v^M with the components of the electron wave function in conduction and valence band, it is immediate to verify how their behaviour reflects the previous considerations.

Further, since in the MEF model the coupling coefficient of conduction and valence band is proportional to ∇V , interband current flow arises only in proximity of the interfaces, when both ψ_c^M and ψ_v^M are not vanishing.

On the other hand, even in absence of an external potential, when no interband transition can occur, the Kane model exhibits a coupling of all the envelope functions. Then, the naive interpretation of the envelope functions which we have ascertained for the MEF model, cannot be directly extended to the Kane model.

References

1. G. Ali, G. Frosali, On quantum hydrodynamic models for the two-band Kane system, 2004 (preprint).
2. G. Ali, G. Frosali and C. Manzini, On the drift-diffusion model for a two-band quantum fluid at zero-temperature, *Ukrainian Math. J.* **57(6)**, 723-730 (2005).
3. G. Borgioli, G. Frosali, P.F. Zweifel, Wigner approach to the two-band Kane model for a tunneling diode, *Transport Theory Stat. Phys.* **32(3&4)**, 347-366 (2003).
4. G. Borgioli, O. Morandi, G. Frosali, and M. Modugno, Different approaches for multi-band transport in semiconductors, *Ukrainian Math. J.* **57(6)**, 742-748 (2005).
5. L. Demeio, L. Barletti, A. Bertoni, P. Bordone and C. Jacoboni, Wigner function approach to multi-band transport in semiconductors, *Physica B*, **314** 104-107 (2002).
6. A. Jünger, *Quasi-hydrodynamic Semiconductor Equations*, Birkhäuser, Basel, 2001.
7. E. O. Kane, Energy band structure in *p*-type Germanium and Silicon, *J. Phys. Chem. Solids* **1**, 82-89 (1956).
8. J. Kefi, *Analyse mathématique et numérique de modèles quantiques pour les semiconducteurs* PhD Thesis, Toulouse University (2003).
9. J. M. Luttinger and W. Kohn, Motion of electrons and holes in perturbed periodic fields, *Phys. Rev.* **97**, 869-883 (1955).

10. M. Modugno, O. Morandi, A multi-band envelope function model for quantum transport in a tunneling diode, *Phys. Rev. B* (2005) (to appear)
11. R.Q. Yang, M. Sweeny, D. Day and J.M. Xu, Interband tunneling in heterostructure tunnel diodes, *IEEE Transactions on Electron Devices*, **38**(3) 442-446 (1991).
12. W.T. Wenckebach, *Essential of Semiconductor Physics*, J.Wiley & Sons, Chichester, 1999.